Spheroid-based engineering of a human vasculature in mice

Abdullah Alajati[1–3,6,7], Anna M Laib[1,7], Holger Weber[2,6,7], Anja M Boos[1,2], Arne Bartol[1], Kristian Ikenberg[2], Thomas Korff[2,6], Hanswalter Zentgraf[4], Cynthia Obodozie[2,6], Ralph Graeser[5], Sven Christian[1,2], Günter Finkenzeller[3], G Björn Stark[3], Mélanie Héroult[1,2] & Hellmut G Augustin[1,2]

The complexity of the angiogenic cascade limits cellular approaches to studying angiogenic endothelial cells (ECs). In turn, *in vivo* assays do not allow the analysis of the distinct cellular behavior of ECs during angiogenesis. Here we show that ECs can be grafted as spheroids into a matrix to give rise to a complex three-dimensional network of human neovessels in mice. The grafted vasculature matures and is connected to the mouse circulation. The assay is highly versatile and facilitates numerous applications including studies of the effects of different cytokines on angiogenesis. Modifications make it possible to study human lymphangiogenic processes *in vivo*. EC spheroids can also be coimplanted with other cell types for tissue engineering purposes.

The US National Cancer Institute has estimated that more than 500 million people will benefit from anti- or proangiogenic therapies in the coming decades[1]. If this projection is to be realized, reliable and robust experimental models are critical to further decipher the angiogenic cascade mechanistically and to validate new angiomanipulatory drugs. Numerous cellular and animal models have been developed toward this end. Cellular assays mimic individual steps of the angiogenic cascade, such as migration or proliferation of ECs or the capillary-like formation of sprouts and tubes in two- or three-dimensional assay systems[2,3]. As such, they are reductionist and to only a limited extent represent a legitimate surrogate for the complexity of angiogenic processes *in vivo*[4]. In turn, the multicellularity of animal models often limits detailed mechanistic interpretation of experimental findings. Moreover, many *in vivo* models are complicated by the contribution of an inflammatory cellular infiltrate that may account for many of the observed discrepancies between developmental (that is genetic) and adult angiogenesis models[2,4–7].

The angiogenic endothelial cell (EC) is at the heart of the angiogenic cascade. The present study was therefore aimed at developing and validating a reliable and robust *in vivo* angiogenesis assay that (i) is based on the use of human ECs as primary experimental input, variable and readout; (ii) mimics the complexity of the angiogenic cascade, with sprouting, anastomosing assembly, maturation and perfusion; (iii) is easily accessible for quantitative analyses; and (iv) is flexible and versatile enough to facilitate multiple applications. We had previously observed that spheroids of cultured ECs can be embedded in a collagen matrix to serve as focal starting points of outgrowing capillary sprouts[3]. Similarly, we hypothesized that spheroids of ECs might be used as a delivery device for EC transplantation in a suitable gel matrix *in vivo*. Pilot experiments showed this approach to be surprisingly efficacious: as few as 100,000 human ECs (grafted as 1,000 spheroids) were capable of growing a complex three-dimensional capillary network in less than 20 d. Later experiments were therefore aimed at solidly validating the assay and probing its versatility for a number of different experimental applications. The study has led to the establishment of a simple and robust spheroid-based EC implantation assay that can be exploited for numerous angiogenesis- and lymphangiogenesis-related uses.

RESULTS

Human vascular network formation from grafted EC spheroids

Cell-cell contacts are the minimum requirement to render ECs responsive to the activities of survival factors[8]. Correspondingly, spheroidal aggregation prevents EC apoptosis and stabilizes the cells[8]. Hence, we embedded 1,000 spheroids of 100 human umbilical vein endothelial cells (HUVECs) each (corresponding to a surface area of approximately 2.5 cm^2 cultured cells) in a Matrigel-fibrin matrix containing the growth factors VEGF and FGF-2 and subcutaneously implanted these into severe combined

[1]Joint Research Division Vascular Biology of the Medical Faculty Mannheim (CBTM), University of Heidelberg, Ludolph-Krehl-Str. 11-14, D-68167 Mannheim, Germany, and the German Cancer Research Center (DKFZ), Im Neuenheimer Feld 581, D-69120 Heidelberg, Germany. [2]Department of Vascular Biology and Angiogenesis Research, Tumor Biology Center, Breisacher Str. 117, D-79108 Freiburg, Germany. [3]Department of Plastic and Hand Surgery, University of Freiburg Medical Center, Hugstetter Str. 55, D-79106 Freiburg, Germany. [4]Electron Microscopy Group, German Cancer Research Center (DKFZ), Im Neuenheimer Feld 280, D-69120 Heidelberg, Germany. [5]ProQinase GmbH, Breisacher Str. 117, D-79108 Freiburg, Germany. [6]Present addresses: Friedrich-Miescher Institute, Maulbeerstrasse 66, CH-4058 Basel, Switzerland (A.A.); ProQinase GmbH, Breisacher Str. 117, D-79108 Freiburg, Germany (H.W., C.O.); Department of Physiology, University of Heidelberg, Im Neuenheimer Feld 581, D-69120 Heidelberg, Germany (T.K.). [7]These authors contributed equally to this study. Correspondence should be addressed to H.G.A. (augustin@angiogenese.de).

RECEIVED 28 JANUARY; ACCEPTED 13 MARCH; PUBLISHED ONLINE 6 APRIL 2008; DOI:10.1038/NMETH.1198

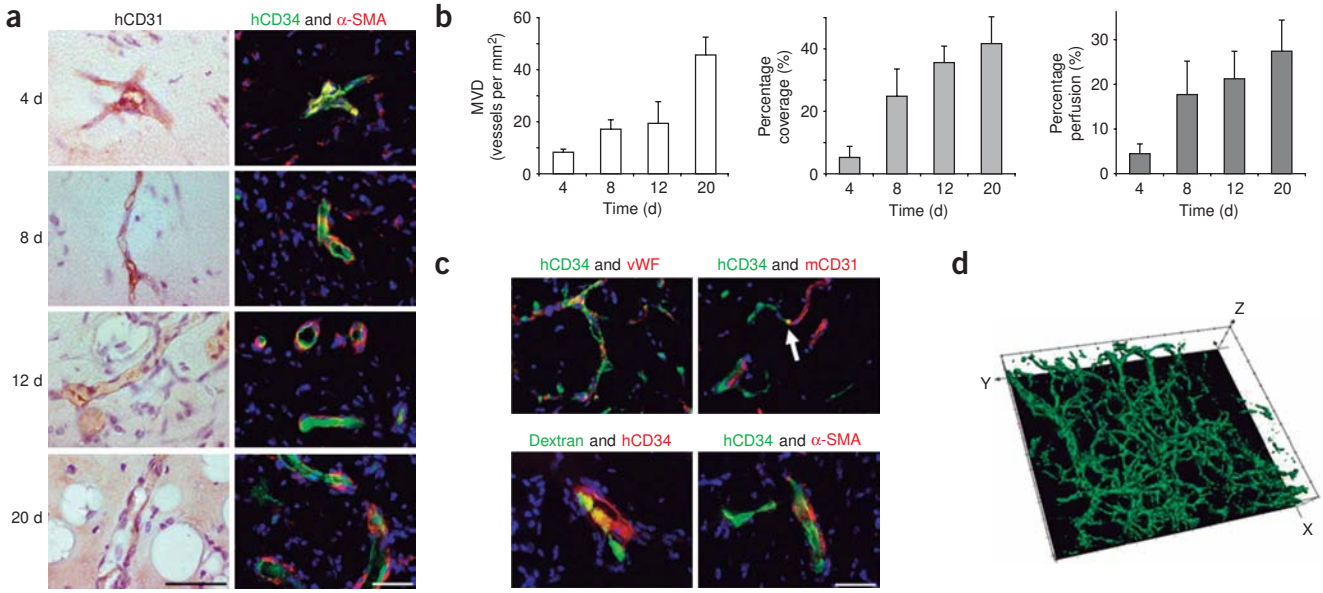

Figure 1 | Characteristics of human neovasculature originating from transplanted EC spheroids. (**a**) Temporal analysis of human neovessel formation after subcutaneous injection of HUVEC spheroids in a Matrigel-fibrin matrix containing VEGF and FGF-2. Immunoperoxidase staining of human CD31 (hCD31)-positive grafted HUVECs with hematoxylin counterstain and a double immunofluorescence staining for grafted HUVECs with human CD34 (green) and mouse α-smooth muscle actin (α-SMA; red). Nuclei were counterstained with Hoechst 33258. Scale bar, 50 μm. (**b**) Quantification of MVD, percentage of mural cell coverage (human CD34 (hCD34)-positive vessels that colocalize with α-SMA–positive host mural cells) and percentage of perfusion (hCD31-positive vessels containing RBCs) over time. The results are mean values ± s.d. for MVD and mural cell coverage and mean ± s.e.m. for perfusion analysis ($n = 5$). (**c**) Characterization of the human vascular network *in vivo* 20 d after implantation. Fluorescence microscopy images of a staining for vWF and human CD34 (hCD34; top left) and for mouse CD31 (mCD31) and hCD34 (top right). Mice were intravenously injected with FITC-dextran and the sections were immunofluorescence stained for hCD34 (bottom left). HAEC spheroids were injected and human vessel formation was analyzed using immunohistochemical staining for hCD34 and α-SMA (bottom right). Nuclei in all images were counterstained with Hoechst 33258. Scale bar, 50 μm. (**d**) Three-dimensional structure of the human neovasculature as assessed by confocal microscopy using immunofluorescence whole-mount staining for hCD31 of a plug implanted for 20 d (slice 0.78 μm, *z* axis 36.5 μm).

immunodeficiency (SCID) mice. We dissected implants of spherical geometry approximately 1 cm in diameter and 2–3 mm in height after 4, 8, 12 and 20 d and analyzed them for the formation of a human EC–derived neovasculature using antibodies to human CD31, CD34 and von Willebrand factor (vWF) to visualize transplanted ECs and antibodies to α-smooth muscle actin (α-SMA) to detect recruited mouse mural cells. Human EC–lined tubes were visible within 4 d of implantation, when mural cell recruitment could not yet be observed (**Fig. 1a**,**b**). The outgrowing human vasculature formed anastomoses with the mouse vasculature (**Fig. 1c**), and perfused vessels (as evidenced by the presence of mouse erythrocytes (**Fig. 1a**) or injected FITC-dextran (**Fig. 1c**)) were detectable after 8 d (**Fig. 1b**). At that time, 24% of growing neovessels had recruited host-derived mural cells (**Fig. 1b**). The human vascular network grew from 25 to 45 vessels per mm^2 between 12 d and 20 d, when 28% of vessels were perfused and more than 40% of them were covered by mural cells (**Fig. 1b**). Whole-mount staining and confocal three-dimensional image assembly revealed a dense network of human vessels of different caliber (**Figs. 1d** and **2a**). The resulting implant vasculature consisted almost exclusively of human ECs, with very limited invasion of mouse ECs (**Fig. 2a**). Ultrastructural analysis confirmed the formation of functional microvessels, which contained erythrocytes, were covered by mural cells and established electron-dense junctional cell-cell contacts (**Fig. 2b**). The resulting vasculature was stable for at least 60 d and responded to exogenous cytokines. For example, local injection of tumor necrosis factor α (TNF-α) readily led to the expression of inducible EC adhesion molecules such as ICAM-1 and VCAM-1 (**Supplementary Fig. 1a** online). Correspondingly, the newly formed blood vessels supported the recruitment of injected dye-labeled human monocytic U937 cells after stimulation with TNF-α. (**Supplementary Fig. 1b**). The assay had been optimized for use with HUVECs. However, other populations of differentiated human ECs were similarly able to form functional neovasculatures upon xenotransplantion in immunocompromized mice. These included aortic endothelial cells (HAECs) (**Fig. 1c**), dermal microvascular endothelial cells (HDMECs), saphenous vein endothelial cells (HSVECs) and umbilical artery endothelial cells (HUAECs) (**Supplementary Fig. 2** online).

We have developed the EC spheroid implantation technique as an experimental model for studying vessel formation originating from gain-of-function- or loss-of-function-manipulated endothelial cells to assess new candidate molecules of the angiogenic cascade. We consequently established retrovirally transduced HUVECs expressing luciferase to probe the feasibility of studying manipulated primary human ECs in the assay and to develop a technique for the noninvasive tracing of neovascularization of grafted human ECs. Luciferase-expressing HUVECs evenly vascularized the Matrigel-fibrin gel and formed a vascular network made up of human endothelial cells that was stable for at least 40 d (**Fig. 2a**). Bioluminescence imaging facilitated the noninvasive visualization of grafted HUVECs (**Fig. 2c**).

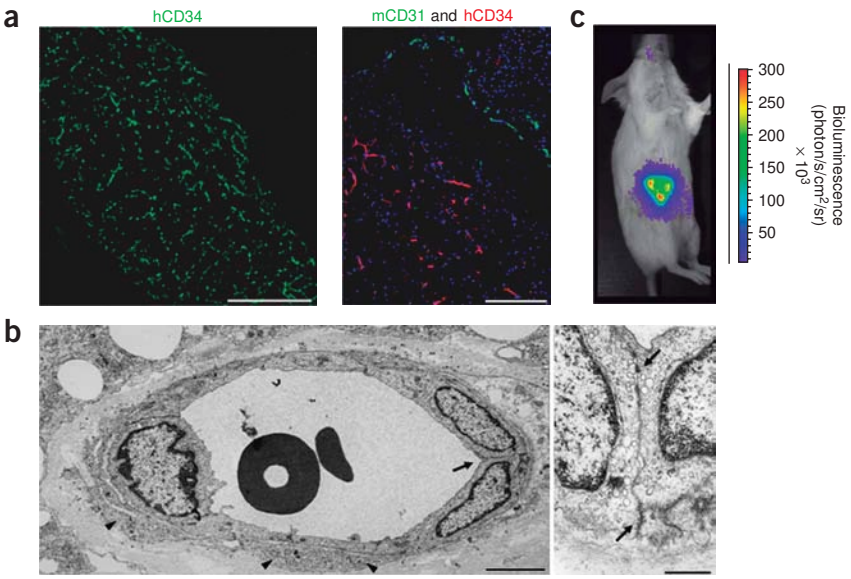

Figure 2 | Vascularization originating from luciferase-expressing HUVEC spheroids in a Matrigel-fibrin matrix containing VEGF and FGF-2 subcutaneously injected into SCID mice. (**a**) Representative immunofluorescence images of human CD34 (hCD34)-positive neovessels in a HUVEC Matrigel-fibrin plug (scale bar, 500 μm) and of human CD34-positive (hCD34) and mouse CD31-positive (mCD31) vessels (scale bar, 200 μm). (**b**) Electron microscopy images of a blood vessel in the center of the grafted plug that is covered by mural cells (arrowheads), contains intraluminal erythrocytes and has junctional cell-cell contacts (arrow). Scale bar, 3 μm. Magnification of a cell-cell contact with a tight junction–like electron-dense zone (arrows). Scale bar, 0.5 μm. The electron microscopic analysis does not formally identify the vessels in the plug as originating from the grafted human ECs, yet the central plug vessels are solely of human origin (**a**). (**c**) The formation of a human vasculature was noninvasively monitored by bioluminescence imaging 40 d after implantation of luciferase-expressing HUVECs. sr, steradian.

Differences between VEGF- and FGF-2-induced angiogenesis

We next probed the feasibility and robustness of the spheroidal EC transplantation technique as a qualitative and quantitative angiogenesis assay by studying the activities of individual angiogenic cytokines. Both VEGF and FGF-2 are potently angiogenic *in vivo*[9,10]. VEGF has been solidly established as a specific, hierarchically high inducer of the angiogenic cascade, whereas FGF-2 is a more pleiotropic growth factor[10]. When individually applied, both growth factors proved to be effective inducers of capillary sprouting originating from transplanted HUVEC spheroids. FGF-2 stimulation induced the formation of a perfused, mural cell–covered neovasculature (**Fig. 3a**, **Supplementary Fig. 3** online). In contrast, VEGF stimulation led to the formation of a tip cell–rich, non-perfused endothelial network with numerous filopodial extensions that was poorly covered by mural cells (**Fig. 3a**, **Supplementary Fig. 3**). Quantification of the resulting microvessel densities revealed that VEGF and FGF-2 had similar potencies and had an additive effect when administered together (**Fig. 3b**).

Long-term application of VEGF in the context of a complex organ microenvironment has previously been shown to lead to the formation of durable blood vessels[11]. Yet, VEGF alone did not cause perfused and mural cell–covered blood vessels to grow in the spheroidal EC xenotransplantation assay, suggesting that other factors or microenvironmental conditions may be required to enable VEGF to induce the growth of mature blood vessels. Co-stimulation with VEGF and PDGF-BB abrogated the tip cell phenotype and resulted in the formation of perfused, mural cell–covered blood vessels (**Supplementary Fig. 4** online). Likewise, coimplantation of human umbilical artery smooth muscle cells (SMCs) with HUVEC spheroids led to the formation of perfused, mural cell–covered blood vessels after VEGF stimulation (**Supplementary Fig. 4**). Normal human dermal fibroblasts (NHDFs) similarly exerted paracrine effects that enabled VEGF to induce growth of perfused blood vessels (**Supplementary Fig. 4**). These findings demonstrate the feasibility of the assay for the qualitative and quantitative analysis of individual steps of the angiogenic cascade in a relevant *in vivo* model and also provided new insights into the biology of VEGF function.

Antiangiogenic drug validation

Intense efforts are presently underway to develop second-generation antiangiogenic drugs that act synergistically to approved therapies targeting VEGF and the VEGF receptor (VEGFR). To exploit the suitability of the EC spheroid transplantation assay for testing antiangiogenic drugs, we performed prevention and intervention experiments with the VEGF receptor blocker PTK787/ZK222584 (PTK/ZK) (kindly provided by Novartis/Bayer Healthcare)[12]. For prevention trials, PTK/ZK was given twice daily for 20 d starting 1 d after HUVEC spheroid implantation. For intervention trials, grafted human neovessels were allowed to grow for 20 d, after which PTK/ZK was given twice daily for another 20 d. PTK/ZK completely blocked VEGF-induced angiogenesis in the prevention trial and caused regression of more than 50% of neovessels in the intervention trial (**Fig. 4a**,**b**), demonstrating the sensitivity of an established but immature VEGF-induced vasculature to anti-VEGFR therapies. To study the effect of antiangiogenic therapy on a more mature neovasculature, we probed the effect of PTK/ZK in VEGF and FGF-2 co-stimulation experiments. PTK/ZK significantly inhibited VEGF- and FGF-2-induced angiogenesis in the prevention trial ($P < 0.05$). However, it had only limited efficacy in the intervention trial, producing no significant difference in microvessel density (MVD) between the control and the experimental groups (**Fig. 4c**,**d**). Yet there was a significant difference when non-mural-cell-covered microvessel densities were simply compared between the control group and the VEGF and FGF-2 intervention trial group ($P < 0.02$) (**Fig. 4d**). These experiments validate the assay for antiangiogenic drug screening purposes and demonstrate its usefulness in relating experimental findings to individual steps of the angiogenic cascade.

Growth of lymphatic vessels from LEC spheroids

Blood endothelial cells (BECs) and lymphatic endothelial cells (LECs) have in recent years been cellularly and molecularly

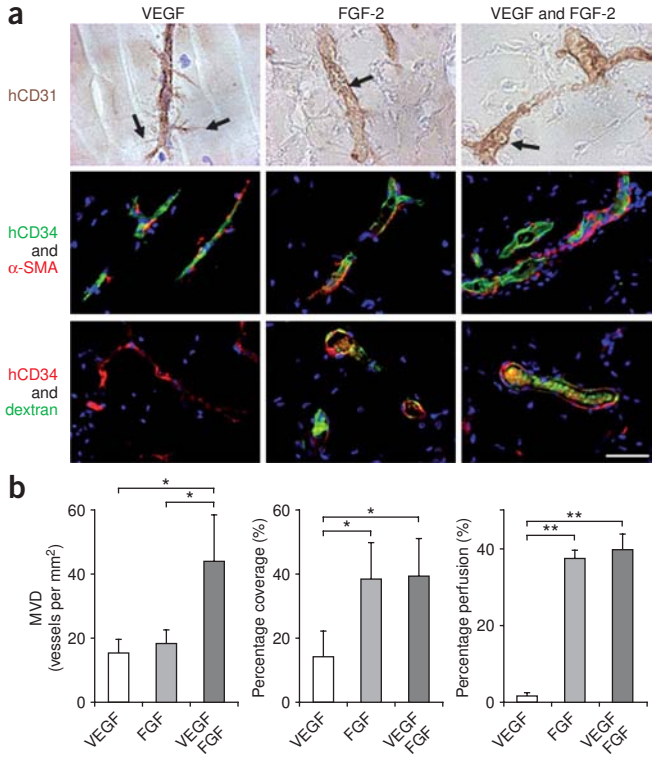

Figure 3 | Analysis of VEGF- and FGF-2–induced angiogenesis. (**a**) Morphological analysis of human neovessel formation after subcutaneous injection of HUVEC spheroids in a Matrigel-fibrin matrix containing VEGF, FGF-2 or both 20 d after implantation. Immunoperoxidase detection of human CD31 (hCD31)-positive cells with hematoxylin counterstain (top), immunofluorescence double staining for human CD34 (hCD34; green) and α-SMA (red) (middle), and immunofluorescence staining for hCD34 (red) with detection of intravenously injected FITC-dextran (green) (bottom). Nuclei were counterstained with Hoechst 33258. Scale bar, 50 μm. (**b**) Quantification of MVD, mural cell coverage and perfusion (as described in **Fig. 1b**). Asterisks denote statistically significant differences (*$P < 0.05$, **$P < 0.001$) between the indicated pairs. The results are mean values ± s.d. ($n = 3$).

characterized as distinctly different lineages of endothelial cells[13]. We therefore hypothesized that the spheroid transplantation technique developed for BECs might similarly be adapted to grow human lymphatics in mice from grafted human LEC spheroids (1,500 spheroids of 200 cells each). Implantation of purified, uniformly podoplanin-positive LEC spheroids led to the formation of CD31-positive vascular structures (**Fig. 5a**). Yet less than 50% of these expressed the lymphatic marker podoplanin 20 d after implantation (**Fig. 5a**,**b**). We therefore pursued coimplantation experiments to generate microenvironmental conditions that better maintain the LEC phenotype. Coimplantation of LECs with human fibroblasts resulted in the formation of more than 90% podoplanin-positive vessels (**Fig. 5a**,**b**). The identity of engineered lymphatic vessels was also confirmed by immunohistochemistry using an antibody against Lyve1 (**Fig. 5c**). Electron microscopy revealed typical lymphatic structures with intercellular gaps and numerous endocytotic vesicles (**Fig. 5d**). This experimental approach allows functional experiments *in vivo*, the study of the lymphangiogenic potential of different LEC populations and the mechanistic study of LEC differentiation. Yet, unlike the perfused BEC vasculature, LEC networks did not connect to host lymphatics (for example, there was no clearance of injected dye).

Use of EC spheroids for tissue engineering applications

After establishing a robust assay to engineer a patent humanized vasculature in mice, we set up a proof-of-principle experiment aimed at probing the feasibility of using grafted human EC spheroids for tissue engineering. Coimplantation of osteoblast

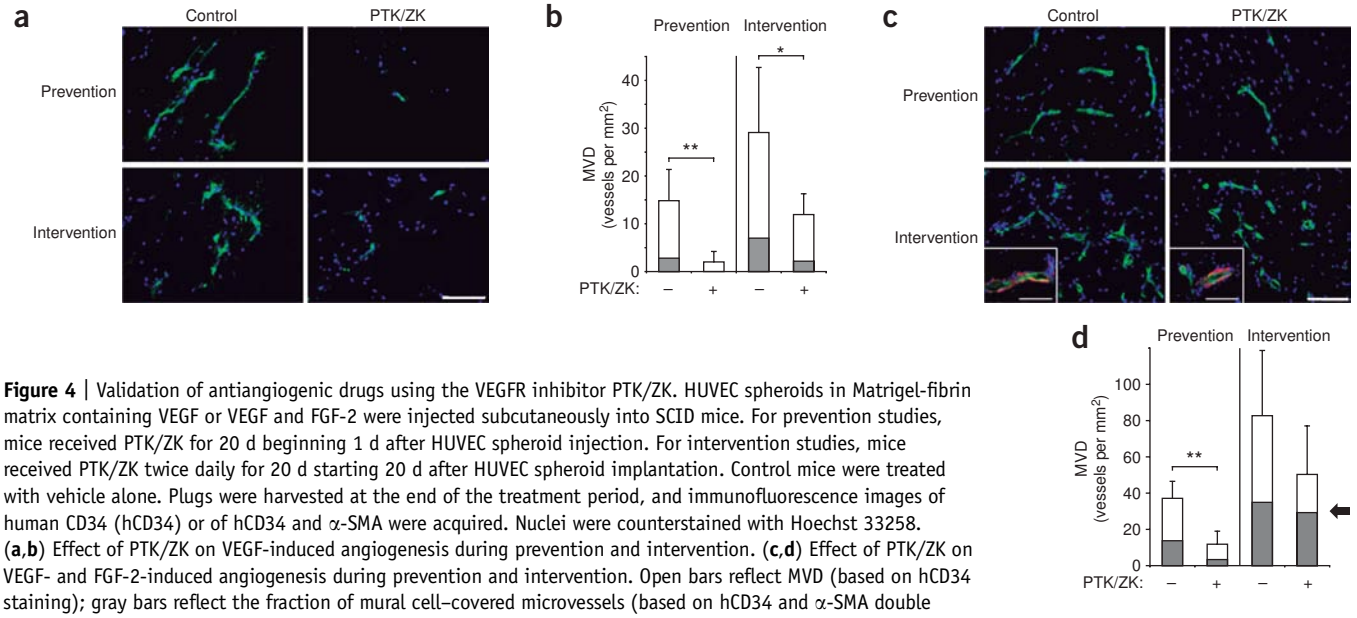

Figure 4 | Validation of antiangiogenic drugs using the VEGFR inhibitor PTK/ZK. HUVEC spheroids in Matrigel-fibrin matrix containing VEGF or VEGF and FGF-2 were injected subcutaneously into SCID mice. For prevention studies, mice received PTK/ZK for 20 d beginning 1 d after HUVEC spheroid injection. For intervention studies, mice received PTK/ZK twice daily for 20 d starting 20 d after HUVEC spheroid implantation. Control mice were treated with vehicle alone. Plugs were harvested at the end of the treatment period, and immunofluorescence images of human CD34 (hCD34) or of hCD34 and α-SMA were acquired. Nuclei were counterstained with Hoechst 33258. (**a**,**b**) Effect of PTK/ZK on VEGF-induced angiogenesis during prevention and intervention. (**c**,**d**) Effect of PTK/ZK on VEGF- and FGF-2-induced angiogenesis during prevention and intervention. Open bars reflect MVD (based on hCD34 staining); gray bars reflect the fraction of mural cell–covered microvessels (based on hCD34 and α-SMA double staining; inset in **c**). The arrow in **d** marks the selective regression of the neovasculature not covered by mural cells in the VEGF and FGF-2 intervention trial. The results are mean values ± s.d. ($n = 7$–9 per experimental group). Asterisks denote statistically significant differences (*$P < 0.05$, **$P < 0.001$) between the indicated pairs. Scale bar, 50 μm.

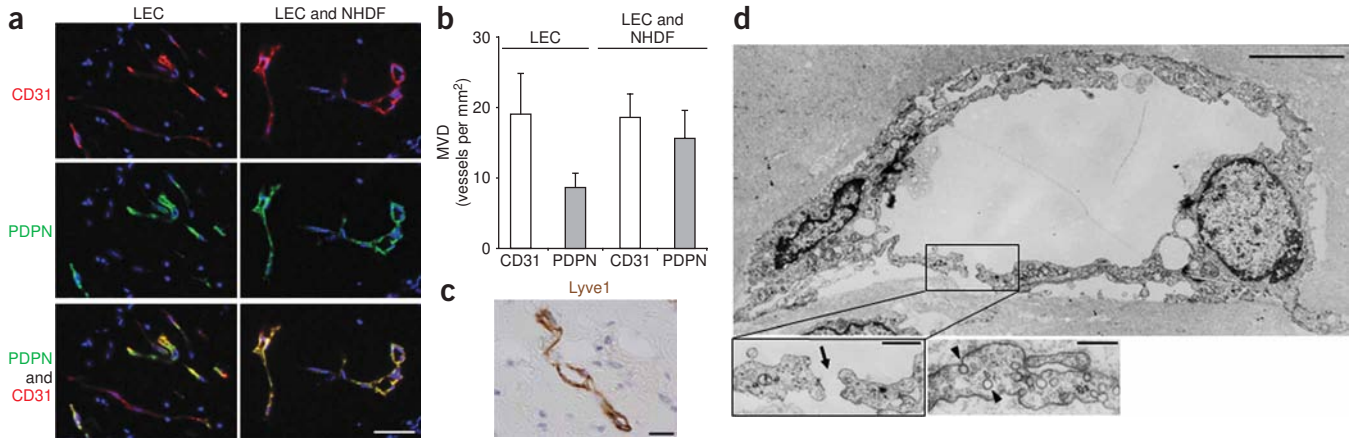

Figure 5 | Growth of lymphatic vessels from podoplanin-positive LECs grafted as spheroids in a Matrigel-fibrin matrix. (**a**) LEC spheroids were grafted in a Matrigel-fibrin matrix containing VEGF, FGF-2 and VEGF-C or were implanted in the presence of dispersed NHDF in the presence of growth factors (VEGF, FGF-2 and VEGF-C). Plugs were harvested after 20 d and sections were double immunofluorescence stained for human CD31 (hCD31; red) and human podoplanin (PDPN; green). Nuclei were counterstained with Hoechst 33258. Scale bar, 100 μm. (**b**) Quantification of MVD (number of hCD31- and PDPN-positive vessels per mm^2). The results are mean values ± s.e.m. ($n = 5–7$ per experimental group). (**c**) Light microscopy image of an immunoperoxidase staining of human Lyve1-positive lymphatics with hematoxylin counterstain. Scale bar, 20 μm. (**d**) Electron microscopy images of a luminized human lymphatic vessel with open junctions and numerous endocytotic vesicles. Scale bar, 5 μm. Insert, magnification of an open lymphatic junction (arrow). Scale bar, 1 μm. Higher-power view of LEC endocytotic vesicles (arrowheads). Scale bar, 300 nm.

spheroids with HUVEC spheroids led to the formation of grafted human EC–derived, host mural cell–covered blood vessels that were interspersed among the outgrowing osteoblasts (**Supplementary Fig. 5a,c** online). Quantification of vessel formation revealed a similar microvessel density in endothelial and osteoblast coimplants as in endothelial cell monoimplants (**Supplementary Fig. 5b**). Differentiation of osteoblasts was confirmed by staining against osteonectin as well as for calcium deposits using alizarin red S (**Supplementary Fig. 5c**).

DISCUSSION

Different experimental avenues have been taken for the engineering of functional blood vessels *in vivo*. These include (i) the transplantation of *in vitro*–preformed vascular constructs[14]; (ii) the use of life-extended or immortalized ECs (for example, through Bcl-2 or telomerase transfection)[15,16]; (iii) the coimplantation of ECs with other cell populations[17–20]; (iv) the embedding of ECs into matrix scaffolds such as Matrigel, macroporous hydrogel or polycaprolactone[17,19,21–24]; and (v) the formation of vascular constructs from endothelial progenitor cells or from embryonic stem cell–derived endothelial cells[25–27]. All of these approaches have solidly established the proof of principle that functional and durable blood vessels can be engineered *in vivo*. Yet none of the techniques has proven sufficiently robust and practical to receive widespread application. Nevertheless, a universal and highly versatile experimental protocol for the growth of human blood vessels *in vivo* would be of great use for numerous applications in the fields of vascular research and regenerative medicine. We have developed a quantitative spheroid-based EC transplantation technique for the formation of durable and perfused vascular networks *in vivo* (**Supplementary Fig. 6** online). The principle of this assay relies on the fact that spheroidal aggregation stabilizes ECs and renders them responsive to the activities of survival factors[8]. As such, EC spheroids can be used as focal starting points for the sprouting of capillaries. Spheroidal delivery of ECs facilitated the generation of a complex vascular network from as few as 100,000 cells (corresponding to a surface area of approximately 2.5 cm^2 cultured cells) (**Fig. 1d**). The high efficacy of the assay was also due to the use of a mixture of Matrigel and fibrin (1:1), a matrix that proved empirically superior to single collagen, Matrigel or fibrin matrices. Most notably, the addition of fibrin to Matrigel circumvented the necessity of adding heparin for the retention of growth factors and took advantage of the release kinetics and longer-lasting effects of fibrin-immobilized angiogenic growth factors[28].

The system's versatility proved useful in a number of different applications. We observed that VEGF could grow vascular networks that were not perfused and did not recruit mural cells. These findings support the notion that VEGF is a hierarchically high inducer of the angiogenic cascade that is nevertheless not, on its own, capable of inducing later steps of the angiogenic cascade.

Our angiogenesis prevention and intervention experiments with the VEGFR inhibitor PTK/ZK demonstrated the power of the assay to quantitatively and mechanistically dissect individual steps of the angiogenic cascade (for example, sprouting angiogenesis versus vessel maturation). As such, the assay will prove highly useful for the validation of new antiangiogenic agents and the establishment of combination therapies with established anti-VEGF therapies. This applies particularly to biological therapeutics (such as antibodies and ligand traps) that cannot be studied in mice because of their specificity for human targets.

The rapidly growing field of lymphangiogenesis research has important implications for tumor progression, edema and metabolic diseases[29] and is in urgent need of relevant experimental models. Here we grafted human LEC spheroids as monocultures or coimplanted them with fibroblast. These experiments validated the suitability of the spheroidal grafting technique for growing lymphatic vessels *in vivo*. They also revealed a crucial role of coimplanted fibroblasts in maintaining the differentiated LEC

phenotype, which raises questions about the paracrine microenvironmental requirements that maintain the LEC versus BEC phenotype.

ECs have a high degree of plasticity. It is noteworthy that macrovascular ECs have, in the present study, been successfully used to form durable microvascular capillary networks. The exploitation of the EC spheroid transplantation technique for tissue engineering purposes may provide a unique and versatile experimental approach to robustly induce the neovascularization of grafted tissue constructs, which has hitherto been one of the most critical obstacles in tissue engineering applications. Vascularization from the surrounding tissue is a slow process, underlining the necessity of developing robust delivery techniques to include ECs directly into the grafted tissue[30]. The present study has provided a proof of concept for the feasibility of grafting osteoblasts as spheroids coembedded with EC spheroids in osteoinductive and angioinductive microenvironmental conditions.

The EC spheroid transplantation assay offers numerous applications for the field of vascular research and beyond. The simplicity and robustness of the assay promise to make it a versatile tool to study ECs (**Supplementary Fig. 6**). We successfully implanted genetically modified ECs that could be traced by noninvasive bioluminescence imaging for up to 40 d *in vivo*. The feasibility of manipulating ECs *ex vivo* before implantation for gain-of-function and loss-of-function studies makes it a very attractive, fast, low-cost prescreening instrument that could precede more laborious and time-consuming whole-animal genetic experimental strategies, facilitating focused mechanistic experimental approaches to the functional analysis of individual candidate molecules.

METHODS

Isolation of lymphatic ECs. Lymphatic endothelial cell isolation was carried out as described earlier[13]. Briefly, polyclonal anti-podoplanin (kindly provided by D. Kerjaschki, Dept. of Clinical Pathology, University of Vienna), MACS colloidal super-paramagnetic MicroBeads conjugated to goat anti–rabbit IgG (Miltenyi Biotech), and MACS MicroBeads separation columns and a MiniMACS separator (both from Miltenyi Biotech), were used for cell isolation according to the manufacturer's protocol.

Generation of EC spheroids. EC spheroids of defined cell number were generated as described previously[3]. In brief, endothelial cells were suspended in corresponding culture medium containing 0.25% (wt/vol) methylcellulose and grown overnight as hanging drops. Under these conditions, all suspended cells contribute to the formation of a single spheroid, of defined cell number, per drop.

Subcutaneous injection of EC spheroids. Spheroids were harvested, washed with EC basal medium (Promocell), centrifuged and mixed in 500 µl Matrigel (growth factor reduced; BD Biosciences) and fibrinogen (final concentration 2 mg/ml; Calbiochem) containing different growth factors (500 ng/ml each) or different cells. Thrombin (0.4 U; Calbiochem) was added to the mixture and injected subcutaneously on each side lateral to the abdominal midline region into 4–6-week-old SCID mice. Mice were killed 4–40 d after implantation and constructs were retrieved and fixed overnight in 4% (wt/vol) paraformaldehyde or in zinc fixative (0.5 g/l calcium acetate, 5 g/l zinc acetate, 5 g/l zinc chloride in 0.1 M Tris, pH 7.4) for immunohistological analysis or in 1:9 (vol/vol) DMSO/methanol for human CD31 whole-mount staining. For perfusion studies, FITC-dextran (100 µl; 70,000 MV, 25 mg/ml, anionic, lysine fixable; Molecular Probes) was injected into the tail veins of mice 20 d after spheroid implantation. Circulation was allowed to continue for 10 min before sacrifice. Constructs were retrieved and fixed overnight in 4% (wt/vol) paraformaldehyde. To study EC responsiveness, 50 µl of TNF-α (2 ng/µl) or saline was injected subcutaneously at the site of the implanted plugs. Noninvasive imaging of the human vasculature was achieved through retroviral transfection of HUVECs with a pLIB-EGFP-IRES-LUCIneo construct. LUC^+ GFP^+ spheroids were mixed in Matrigel-fibrin containing VEGF-A and FGF-2 into SCID mice. Mice were anesthetized 40 d after implantation and the LUC^+ GFP^+ human vasculature was monitored using a CCD camera (NightOWL; Berthold) after intraperitoneal injection of luciferin for 20 min (100 µl, 20 mg/ml; Promega). After imaging was completed, mice were sacrificed and the constructs were retrieved and processed for morphological analysis. All animal experiments of this study were approved by the responsible committees of the Regierungspräsidium Freiburg (G-04/56) and the Regierungspräsidium Karlsruhe (35-9185.81/G-67/06).

Quantification and statistical analysis. All implants were completely sectioned, and three slides were selected from the beginning, the middle and the end of each construct. MVD analysis was done by staining sections for human CD34. Images of the complete matrix area were taken using an Olympus IX50 inverted microscope and assembled by multiple image alignment (Cell-P, Olympus). Fluorescent particles were automatically counted in the matrix area and calculated as vessel number per mm^2. Mural cell coverage was analyzed by double staining of sections for human CD34 and α-SMA, and the fraction of human CD34–positive vessels associated with α-SMA–positive mural cells was counted on three microscopic images (200×). Perfusion analysis was performed by staining one slide per construct for human CD31 and counting host red blood cells (RBCs) containing human vessels in relation to the total number of human vessels in three microscopic fields (200×) per slide (% of perfused vessels). The number of plugs analyzed is given for each experiment (n). All results are expressed as mean ± s.d. (s.d) or mean ± standard error (s.e.m). Differences between experimental groups were analyzed by unpaired Student's t-test, and $P < 0.05$ was considered as statistically significant.

Supplementary methods. Details of cell culture, animals, antibodies, growth factors and reagents, as well as of all morphological, immunohistochemical and electron microscopic analyses, are summarized in the **Supplementary Methods** online.

Note: Supplementary information is available on the Nature Methods website.

ACKNOWLEDGMENTS

This work was supported by grants from the German Research Council (Deutsche Forschungsgemeinschaft, AU83/10-1), the European Union (LSHG-CT-2004-503573), the Austrian Science Fund (FWF S9404-B11), the State of Baden-Württemberg Kompetenznetzwerk Biomaterialien and the Fördergesellschaft der Klinik für Tumorbiologie Freiburg.

AUTHOR CONTRIBUTIONS

A.A., A.M.L., H.W., S.C., M.H., G.B.S. and H.G.A. conceived and designed the experiments. A.A., A.M.L., H.W., A.M.B., A.B., K.I., T.K., H.Z., C.O., R.G., G.F. and M.H. performed experiments. A.A., A.M.L., H.W., M.H., S.C. and H.G.A. contributed to data analysis. A.A., A.M.L., H.W., M.H. and H.G.A. contributed to the writing of the manuscript. All authors discussed and commented on the manuscript.

Published online at http://www.nature.com/naturemethods/
Reprints and permissions information is available online at http://npg.nature.com/reprintsandpermissions

1. National Cancer Institute (USA). Angiogenesis initiative fueling collaboration. *Cancer Bull.* **3** (9), 1–6 (2006).
2. Ausprunk, D.H., Knighton, D.R. & Folkman, J. Vascularization of normal and neoplastic tissues grafted to the chick chorioallantois. Role of host and preexisting graft blood vessels. *Am. J. Pathol.* **79**, 597–628 (1975).
3. Korff, T., Krauss, T. & Augustin, H.G. Three-dimensional spheroidal culture of cytotrophoblast cells mimics the phenotype and differentiation of cytotrophoblasts from normal and preeclamptic pregnancies. *Exp. Cell Res.* **297**, 415–423 (2004).
4. Jain, R.K., Schlenger, K., Hockel, M. & Yuan, F. Quantitative angiogenesis assays: progress and problems. *Nat. Med.* **3**, 1203–1208 (1997).
5. Kenyon, B.M. *et al.* A model of angiogenesis in the mouse cornea. *Invest. Ophthalmol. Vis. Sci.* **37**, 1625–1632 (1996).
6. Norrby, K. In vivo models of angiogenesis. *J. Cell. Mol. Med.* **10**, 588–612 (2006).
7. Passaniti, A. *et al.* A simple, quantitative method for assessing angiogenesis and antiangiogenic agents using reconstituted basement membrane, heparin, and fibroblast growth factor. *Lab. Invest.* **67**, 519–528 (1992).
8. Korff, T. & Augustin, H.G. Integration of endothelial cells in multicellular spheroids prevents apoptosis and induces differentiation. *J. Cell Biol.* **143**, 1341–1352 (1998).
9. Ferrara, N. VEGF and the quest for tumour angiogenesis factors. *Nat. Rev. Cancer* **2**, 795–803 (2002).
10. Presta, M. *et al.* Fibroblast growth factor/fibroblast growth factor receptor system in angiogenesis. *Cytokine Growth Factor Rev.* **16**, 159–178 (2005).
11. Grunewald, M. *et al.* VEGF-induced adult neovascularization: recruitment, retention, and role of accessory cells. *Cell* **124**, 175–189 (2006).
12. Drevs, J. *et al.* Effects of PTK787/ZK 222584, a specific inhibitor of vascular endothelial growth factor receptor tyrosine kinases, on primary tumor, metastasis, vessel density, and blood flow in a murine renal cell carcinoma model. *Cancer Res.* **60**, 4819–4824 (2000).
13. Kriehuber, E. *et al.* Isolation and characterization of dermal lymphatic and blood endothelial cells reveal stable and functionally specialized cell lineages. *J. Exp. Med.* **194**, 797–808 (2001).
14. Rouwkema, J., de Boer, J. & van Blitterswijk, C.A. Endothelial cells assemble into a 3-dimensional prevascular network in a bone tissue engineering construct. *Tissue Eng.* **12**, 2685–2693 (2006).
15. Enis, D.R. *et al.* Induction, differentiation, and remodeling of blood vessels after transplantation of Bcl-2-transduced endothelial cells. *Proc. Natl. Acad. Sci. USA* **102**, 425–430 (2005).
16. Yang, J. *et al.* Telomerized human microvasculature is functional *in vivo*. *Nat. Biotechnol.* **19**, 219–224 (2001).
17. Choong, C.S., Hutmacher, D.W. & Triffitt, J.T. Co-culture of bone marrow fibroblasts and endothelial cells on modified polycaprolactone substrates for enhanced potentials in bone tissue engineering. *Tissue Eng.* **12**, 2521–2531 (2006).
18. Koike, N. *et al.* Tissue engineering: creation of long-lasting blood vessels. *Nature* **428**, 138–139 (2004).
19. Levenberg, S. *et al.* Engineering vascularized skeletal muscle tissue. *Nat. Biotechnol.* **23**, 879–884 (2005).
20. Fischbach, C. *et al.* Engineering tumors with 3D scaffolds. *Nat. Methods* **4**, 855–860 (2007).
21. Ford, M.C. *et al.* A macroporous hydrogel for the coculture of neural progenitor and endothelial cells to form functional vascular networks in vivo. *Proc. Natl. Acad. Sci. USA* **103**, 2512–2517 (2006).
22. Nor, J.E. *et al.* Engineering and characterization of functional human microvessels in immunodeficient mice. *Lab. Invest.* **81**, 453–463 (2001).
23. Skovseth, D.K., Yamanaka, T., Brandtzaeg, P., Butcher, E.C. & Haraldsen, G. Vascular morphogenesis and differentiation after adoptive transfer of human endothelial cells to immunodeficient mice. *Am. J. Pathol.* **160**, 1629–1637 (2002).
24. Skovseth, D.K., Kuchler, A.M. & Haraldsen, G. The HUVEC/Matrigel assay: an in vivo assay of human angiogenesis suitable for drug validation. *Methods Mol. Biol.* **360**, 253–268 (2007).
25. Levenberg, S., Golub, J.S., Amit, M., Itskovitz-Eldor, J. & Langer, R. Endothelial cells derived from human embryonic stem cells. *Proc. Natl. Acad. Sci. USA* **99**, 4391–4396 (2002).
26. Wang, Z.Z. *et al.* Endothelial cells derived from human embryonic stem cells form durable blood vessels *in vivo*. *Nat. Biotechnol.* **25**, 317–318 (2007).
27. Au, P. *et al.* Differential in vivo potential of endothelial progenitor cells from human umbilical cord blood and adult peripheral blood to form functional long-lasting vessels. *Blood* **111**, 1302–1305 (2008).
28. Wong, C., Inman, E., Spaethe, R. & Helgerson, S. Fibrin-based biomaterials to deliver human growth factors. *Thromb. Haemost.* **89**, 573–582 (2003).
29. Alitalo, K., Tammela, T. & Petrova, T.V. Lymphangiogenesis in development and human disease. *Nature* **438**, 946–953 (2005).
30. Eiselt, P. *et al.* Development of technologies aiding large-tissue engineering. *Biotechnol. Prog.* **14**, 134–140 (1998).

Spheroid-based engineering of a human vasculature in mice

Abdullah Alajati, Anna M. Laib, Holger Weber, Anja M. Boos, Arne Bartol, Kristian Ikenberg, Thomas Korff, Hanswalter Zentgraf, Cynthia Obodozie, Ralph Graeser, Sven Christian, Günter Finkenzeller, G Björn Stark, Mélanie Héroult & Hellmut G Augustin

Supplementary figures and text:

Suppl. Figure 1

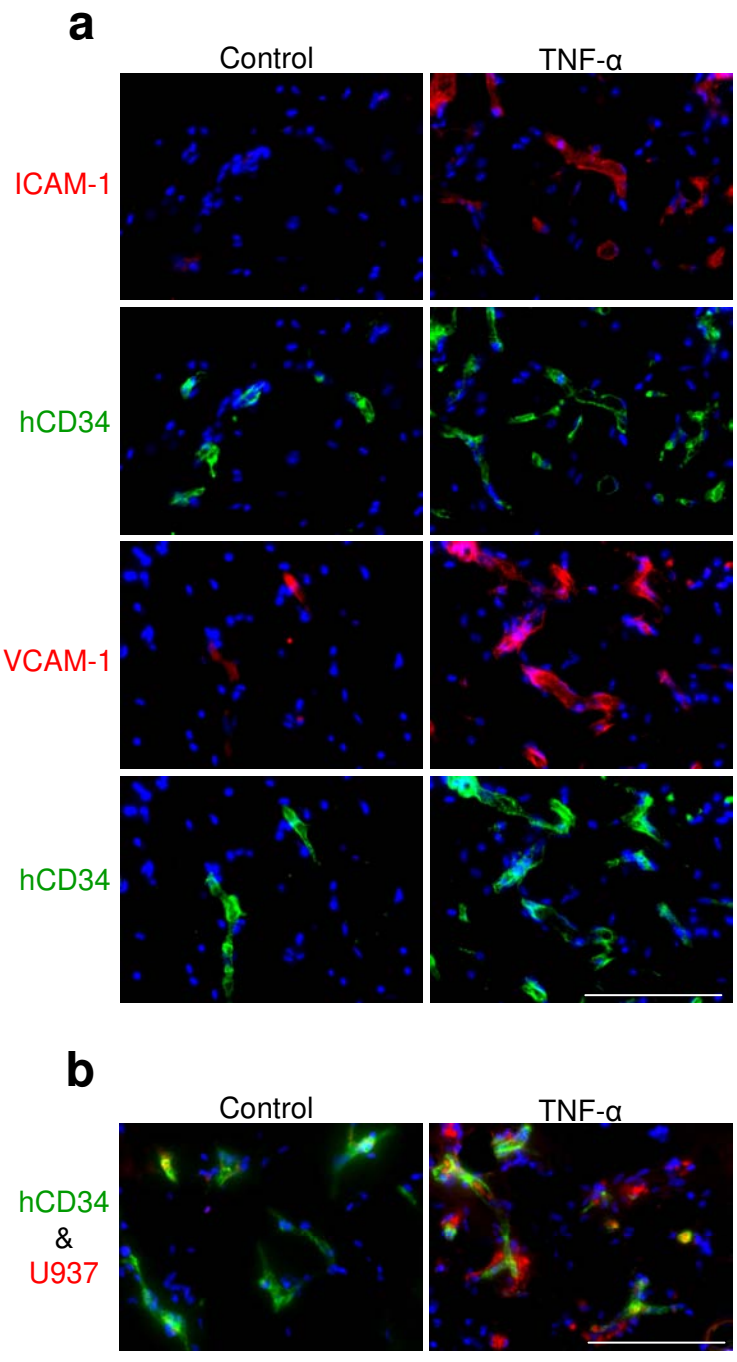

Supplementary Figure 1a,b: Responsiveness of the human grafted vasculature to inflammatory stimulation. HUVEC spheroids (1000 of 100 cells each) were mixed with Matrigel-fibrin containing VEGF and FGF-2 (500ng/ml each) and injected subcutaneously into SCID mice. After 20 days, mice were injected with TNF-α (2ng/µl) into the left flank and saline as control in the right flank of the body. Dye-labelled human U937 monocytes (red fluorescence; Vybrant CM-DiI) were intravenously injected into the tail vein 3 hours after TNF-α stimulation. Mice were sacrificed 1h later and the harvested plugs were analyzed morphologically. Mice were sacrificed 4 h later and the harvested plugs were analyzed morphologically. (**a**) Fluorescence microscopy images of sections, double stained for hICAM-1 and hCD34 or hVCAM-1 and hCD34, respectively. The hCD34 positive human vasculature responded to TNF-α by upregulation of ICAM-1 and VCAM-1 expression. (**b**) Fluorescence microscopy images of a hCD34 staining. Following the injection of labelled U937 cells, the recruitment and extravasation of attracted monocytic cells were directly visualized by detection of red-labelled cells in the vessels and in the matrix. All sections were stained with Hoechst for nuclear detection. Scale bar, 100 µm.

Suppl. Figure 2

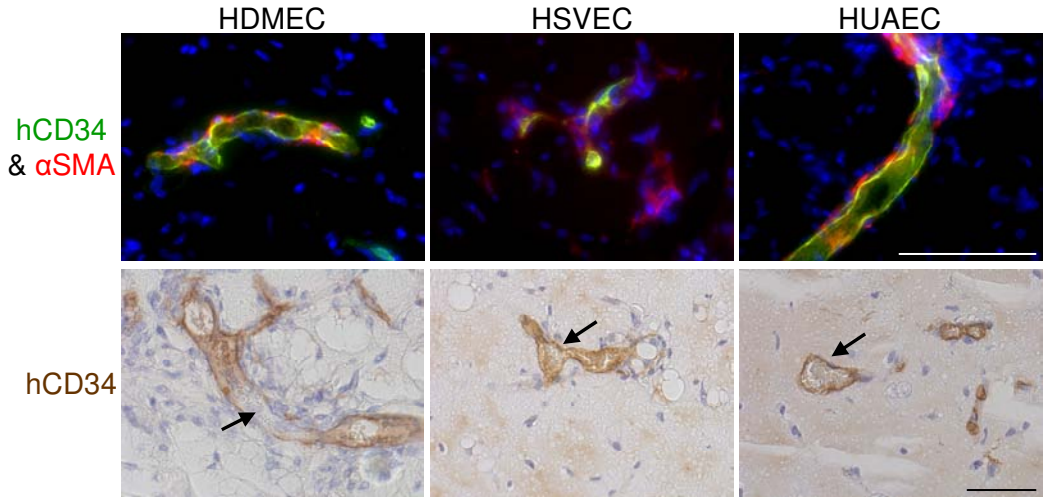

Supplementary Figure 2: Spheroids of different human EC populations give rise to a human vasculature when transplanted into SCID mice. HDMEC-, HSVEC- and HUAEC-spheroids (1000 spheroids, 100 cells each), respectively, were mixed with Matrigel-fibrin matrix containing VEGF and FGF-2 (500 ng each) and injected subcutaneously into SCID mice. Plugs were resected 20 days after implantation. Fluorescence microscopy images of a double staining for hCD34 and α-smooth muscle actin (αSMA; recruited murine mural cells), counterstained with Hoechst for nuclear detection. All tested ECs developed a human capillary network that anastomosed with the mouse vascular system and was covered by mural cells 20 days after implantation. Scale bar, 100 µm. Light microscopy images of an immunohistochemical staining for hCD34 and counterstaining with hemalaun revealed capillary networks carrying erythrocytes (arrows). Scale bar 50 µm.

Suppl. Figure 3

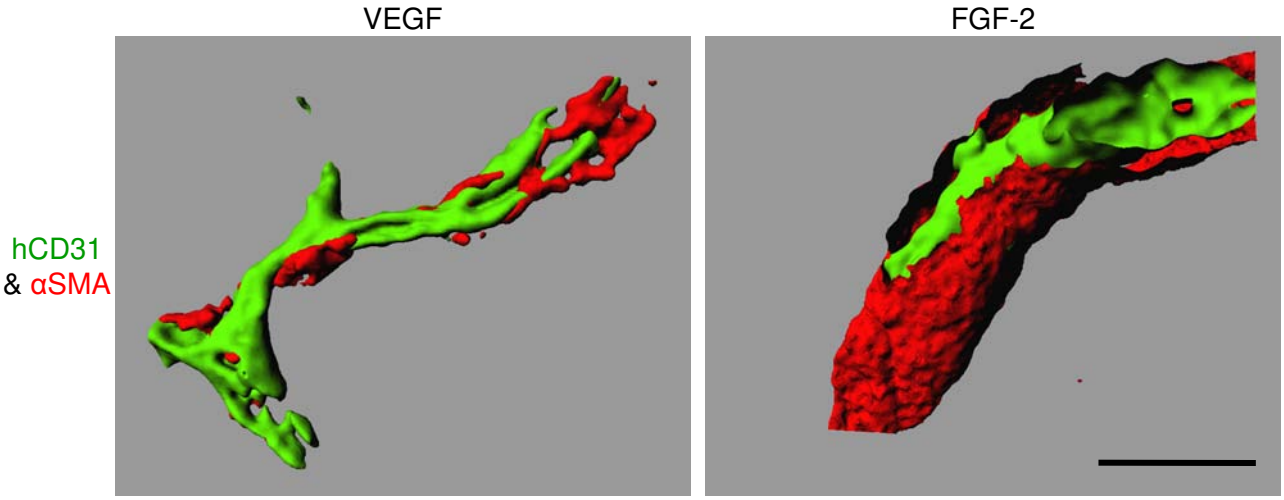

Supplementary Figure 3: Three dimensional analysis of mural cell coverage following VEGF and FGF-2 stimulation. Morphological 3D analysis of human neovessel formation after subcutaneous injection of HUVEC spheroids (1000 of 100 cells each) in a Matrigel-fibrin matrix containing VEGF or FGF-2 into SCID mice. Plugs were resected 20 days after implantation. Sections (20 µm) were immunofluorescence double stained with anti-hCD31 and α-smooth muscle actin (αSMA; recruited murine mural cells). Three dimensional analysis by confocal microscopy, using Imaris 3.1 (3D-software) demonstrated that the newly formed human vasculature was only partly covered by mural cells upon VEGF stimulation. In contrast, FGF-2 stimulation resulted in a nearly complete mural cell coverage of human neovessels. Scale bar, 25 µm.

Suppl. Figure 4

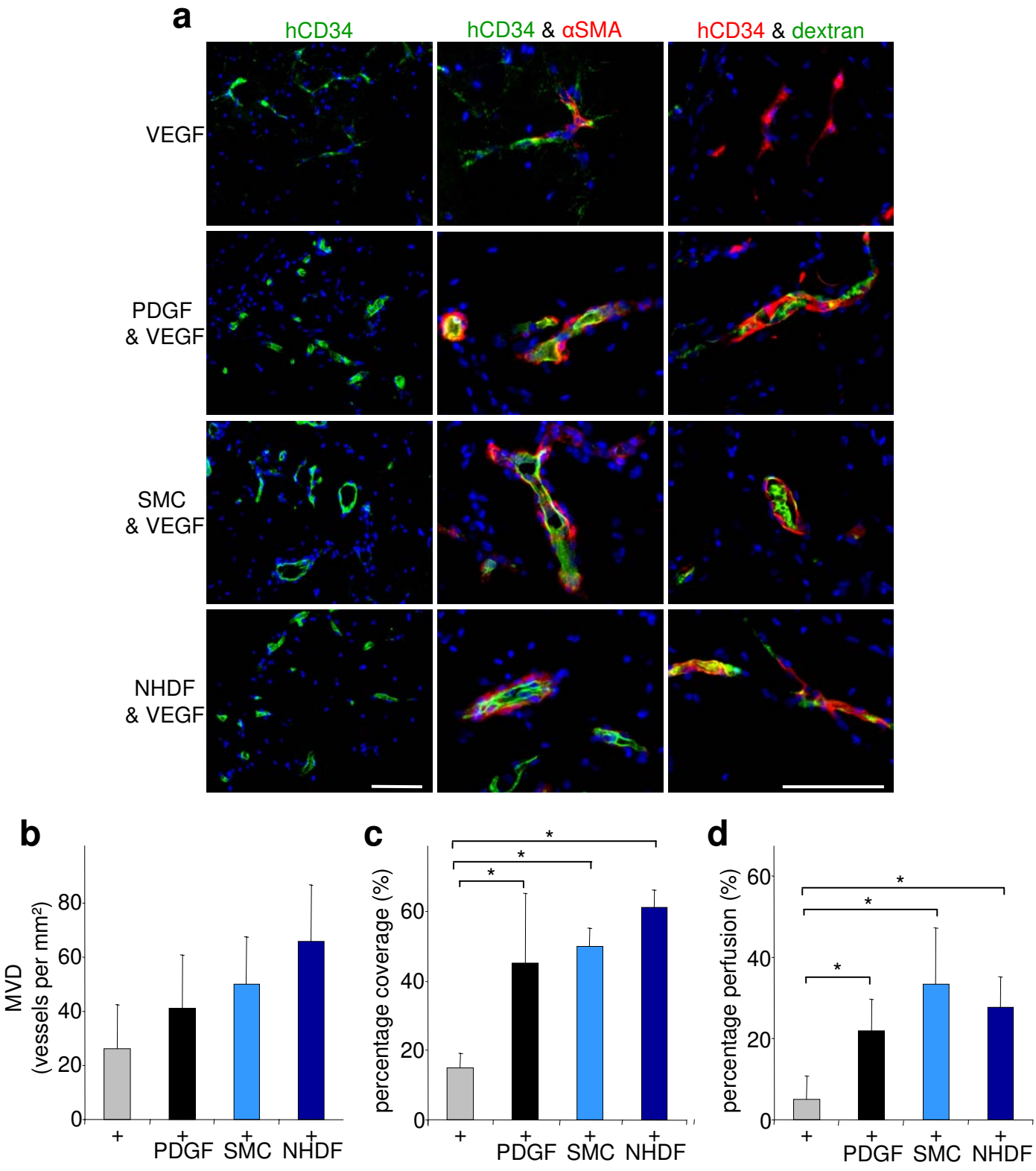

Suppl. Figure 4

Supplementary Figure 4a: Effect of VEGF in combination with PDGF-BB, HUASMC or NHDF on the formation of a human neovasculature originating from xenotransplanted EC spheroids. HUVEC spheroids (1000 of 100 cells each) were subcutaneously injected in a Matrigel-fibrin matrix containing VEGF, VEGF and PDGF-BB, VEGF and HUASMC, or VEGF and NHDF (500ng/ml for VEGF and PDGF-BB, 10^5 cells for HUASMC and NHDF) into SCID mice. Plugs were resected 20 days after implantation. (**a**) Representative fluorescence microscopy images of a hCD34 staining revealed a human vascular network 20 days after subcutaneous injection in all groups. Fluorescence microscopy images of a double staining for hCD34 (grafted HUVEC) and α-smooth muscle actin (αSMA; recruited murine mural cells) revealed only little mural cell coverage in the VEGF stimulated group, whereas VEGF in combination with PDGF, SMC or NHDF resulted in a high degree of mural cell vessel coverage; right: Intravenous injection of FITC-Dextran in combination with immunofluorescence staining of sections for hCD34 revealed a perfused human vasculature in the presence of PDGF, SMC and NHDF. In contrast, stimulation with VEGF alone resulted in non perfused, rarely mural cell covered human vessels. All sections were stained with Hoechst for nuclear detection. Scale bars, 100 µm. (**b**) Quantification of MVD. MVD was quantified by counting the number of hCD34-positive vessels per mm². (**c**) Mural cell coverage was assessed by counting the percentage of hCD34-positive vessels that co-localized with αSMA-positive host mural cells. (**c**) Perfusion was analyzed by counting the percentage of hCD31-positive vessels, containing host RBC. Mural cell coverage as well as perfusion were significantly increased in the presence of PDGF, SMC or NHDF compared to the VEGF alone stimulated group. Stimulation of EC spheroids with VEGF alone was not sufficient to develop a mature human vascular network. The results are mean values ± s.d. ($n = 3$).

Suppl. Figure 5

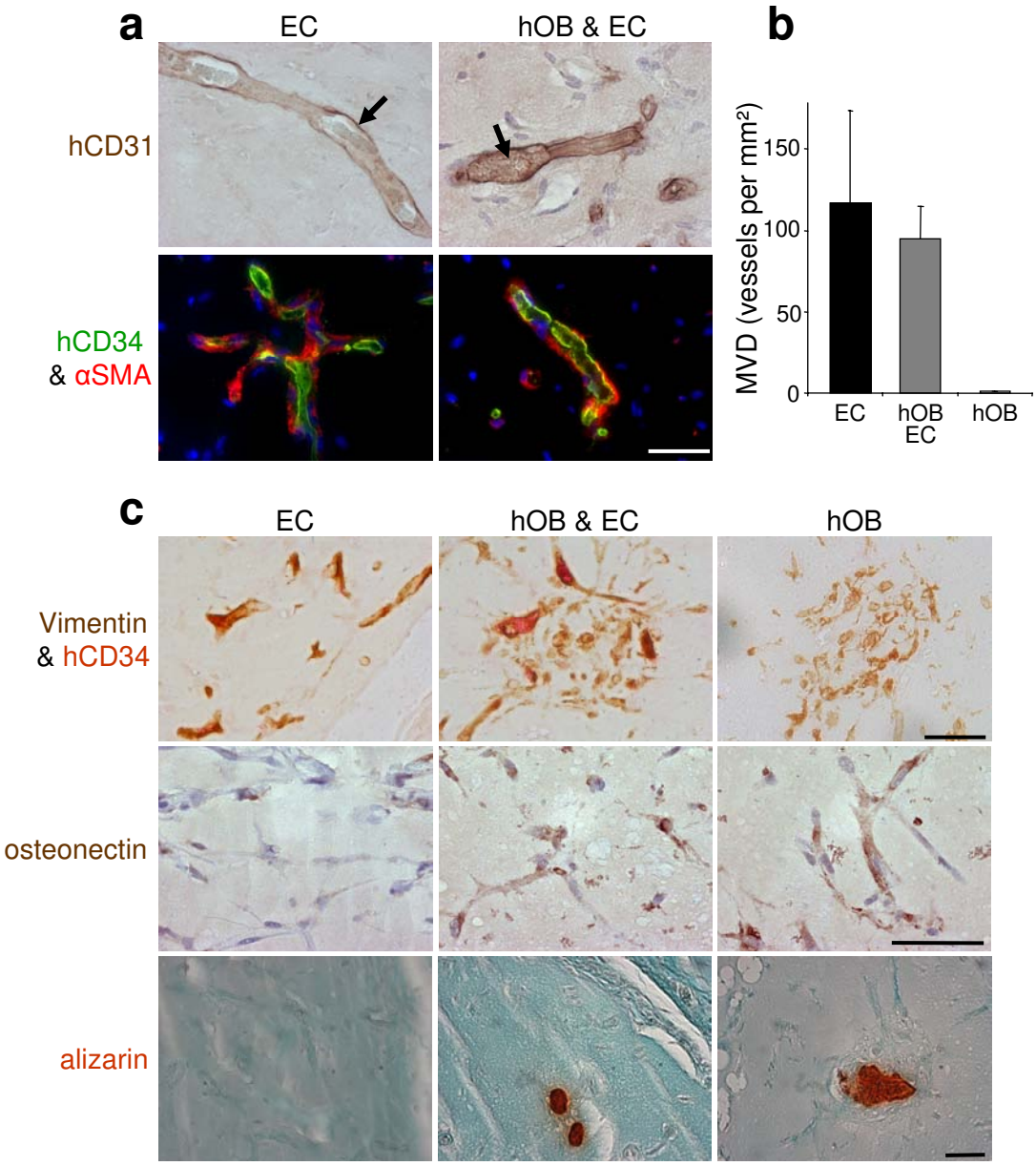

Supplementary Figure 5: Co-implantation of HUVEC spheroids with osteoblasts. (**a**) HUVEC spheroids (500 spheroids; 400 cells per spheroid), mixed co-culture HUVEC and human osteoblast (hOB) spheroids (500 spheroids; 800 cells per spheroid), and hOB spheroids (500 spheroids; 400 cells per spheroid) were mixed in a Matrigel-fibrin matrix containing VEGF and FGF-2 (500 ng/ml each), injected subcutaneously into SCID mice, and incubated for 20 days; (**a)** Light and fluorescence microscopy images of hCD31-positive grafted HUVEC with hematoxylin counterstain and immunofluorescence double staining for hCD34 and αSMA. Nuclei were counterstained with Hoechst. Scale bar, 50 µm. Quantitation of MVD by counting the number of hCD34-positive vessels per mm². The results are mean values ± s.d. (*n* = 3). (**c**) top: Sections were immunohistochemically double stained for hCD34 and hVimentin. Cells with human origin were apparent in the matrix in all constructs. Numerous cells and EC-derived vessels could be detected by hVimentin and hCD34 double staining in constructs with EC spheroids and EC and hOB co-culture spheroids. middle: Detection of Osteonectin in constructs containing hOB co-implanted EC spheroids, but not in mono-implants of EC spheroids. Bottom: Immunohistochemical detection of calcium phosphate with alizarin. The formation of mineral nodules was detected in the constructs containing hOB and co-implanted EC spheroids, whereas no mineral formation could be detected in constructs of EC mono-implants. Scale bar 50 µm.

Suppl. Figure 6

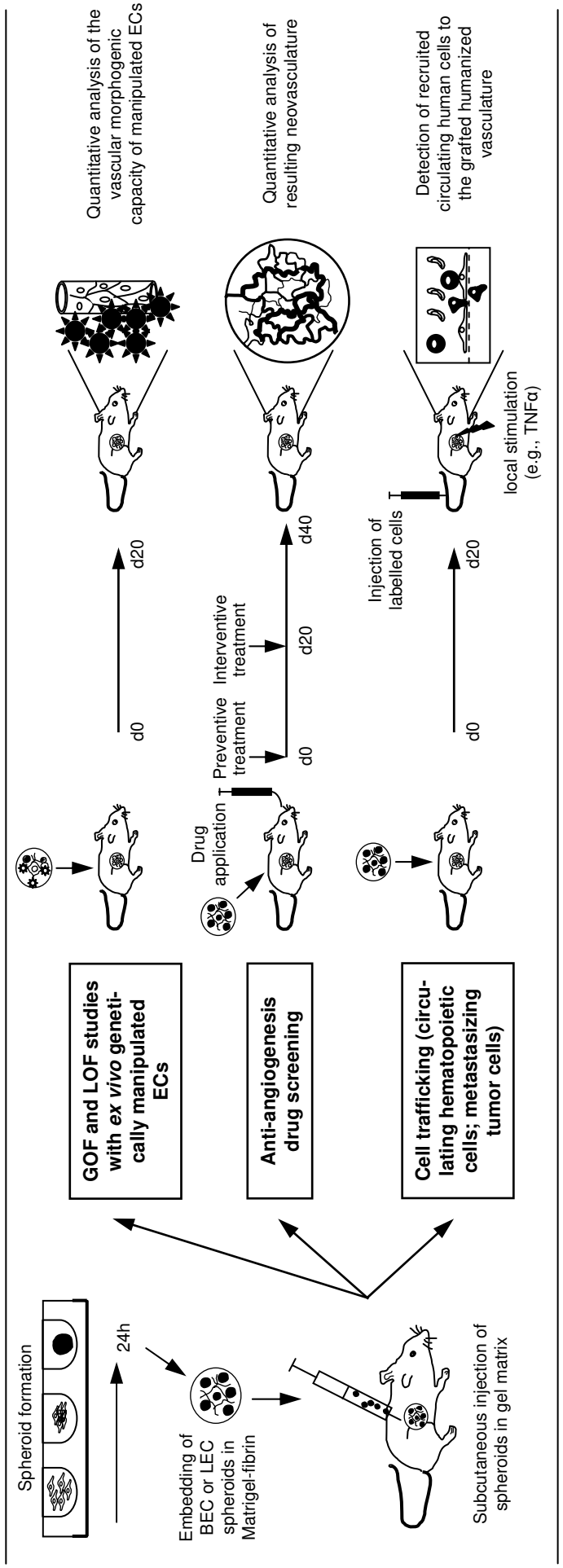

Supplementary Figure 6: Schematic diagram summarizing different applications of the spheroid-based *in vivo* angiogenesis assay (see text for details).

Methods Supplement

Morphological and immunohistochemical analysis

Following fixation with 4% formaldehyde or Zink fixative, Matrigel plugs were embedded in paraffin. Plugs were sectioned at 8 μm, deparaffinized and rehydrated. Anti human CD31 (JC70/A, Dako) and anti human Osteonectin immunohistochemistry was performed using VECTOR M.O.M kit according to the manufacturer's instructions (Vector Laboratories). Anti human CD34/anti mouse CD31 double stainings were performed with paraffin slides that had been digested with Proteinase K at 37°C. Calcium phosphate staining was performed using Alizarin red S solution (Sigma Aldrich Buchs) and counterstained with Fast Green (Merck). For Vimentin, ICAM-1 and VCAM-1 staining, sections were boiled in citrate antigen retrieval buffer (pH 6, Dako); for Lyve-1 in citrate antigen retrieval buffer (pH 9, Dako). Non-specific binding was blocked with 10% goat serum or 7%FCS/1%BSA or 5% donkey or rabbit serum, respectively. Endogenous peroxidases were blocked with 3% H_20_2, followed by avidin/biotin blocking. The following primary antibodies were used: Mouse-αSMA-Cy3 (Sigma Aldrich), mouse-anti-human CD34 (QBEND10, Novocastra), sheep-anti-human CD31 (Dako), rat-anti-mouse CD31 (BD Bioscience), mouse-anti-human Podoplanin (Dako or Abcam), rabbit-anti-human Lyve-1 (RELIATech), goat-anti-human ICAM-1 (R&D Systems), goat-anti-human VCAM-1 (R&D Systems), mouse-anti-human Vimentin (Dako), and mouse-anti-human osteonectin (Biogenex). First antibodies were detected by goat-anti-mouse Alexa Fluor 488 (Invitrogen), donkey-anti-sheep Alexa Fluor 546 (Invitrogen), goat-anti-rat Alexa 488 (Invitrogen), rabbit-anti-goat Alexa Fluor 546 (Invitrogen), goat-anti-mouse conjugated to alkaline phosphatase (Zymed), and biotinylated goat-anti-mouse secondary antibody (Zymed), respectively. Slides were incubated with a streptavidin-peroxidase conjugate (Zymed or Dako) and developed with Fast Red substrate (Dako) or DAB Substrate Chromogen system (Dako). Nuclei were counterstained with Hoechst dye 33258 (Sigma Aldrich) or Meyer's Hemalaun solution (Merck). Slides were examined with an Olympus IX81 microscope. Images were captured with F-View digital camera (Olympus) and processed by Cell F imaging system (Olympus).

Electron microscopy

Specimens were fixed in 2.5% glutaraldehyde buffered with 0.05 M sodium cacodylate. Osmification, dehydration, embedding and sectioning were as described (1). Micrographs were taken with a Zeiss EM-10 electron microscope at 80 kV.

Dextran perfusion

For perfusion studies, 100 µl of FITC conjugated dextran (70,000 MW, 25 mg/ml anionic, Invitrogen) was injected into the tail vein of mice and allowed to perfuse for 10 min. After sacrificing the mice, plugs were retrieved and fixed over night in 4% formaldehyde.

Confocal microscopy

HUVEC-spheroids (1.000 of 100 cells each) were mixed in Matrigel/fibrin matrix containing VEGF-A or FGF-2 (500ng each, R&D Systems) and injected subcutaneously into SCID mice (Harlan Winkelmann). Mice were sacrificed after 20 days. For whole mount staining, plugs were fixed for 24 h in methanol containing 10% DMSO. Thereafter, the plugs were double stained with anti hCD31/αSMA antibodies as described above. The three dimensional structure was analyzed by confocal microscopy using the LSM510 200M laser scanning microscope (Zeiss) and corresponding analyses software Imaris 3.1 (3D-software).

Monocyte (U937) recruitment experiments

TNF-α (50 µl containing 2 ng/µl TNF-α, R&D Systems) or 50 µl saline were injected subcutaneously into the site of a 20 day plug. Human U937 were labeled with red fluorescence solution (Vybrant CM-DiI cell-labeling solution, Invitrogen) according to the manufacturer's instructions. U937 cells (1×10^6) were injected into the mouse tail vein 3 h after TNF-α injection. Mice were sacrificed 1 h after monocyte injection. Plugs were retrieved and fixed in Zinc fixative at 4 C° over night and stained for human CD34 as described above.

Reference

1. Zentgraf, H., & Franke W.W. Differences of supranucleosomal organization in different kinds of chromatin: cell type-specific globular subunits containing different numbers of nucleosomes. *J. Cell Biol.* **99,** 272-286 (1984)